Title

Electronic structure and characterization of a uranyl di-15-crown-5 complex with an unprecedented sandwich structure



Journal

Chemical Communications, 52(86)

ISSN

1359-7345

Authors

Hu, Shu-Xian

Gibson, John K

Li, Wan-Lu

et al.

Publication Date

2016-10-20

DOI

10.1039/c6cc07205d

# Electronic Structure and Characterization of a Uranyl Di-15-Crown-5 Complex

Shuxian Hu,[a] John K. Gibson, [b]* Wan-Lu Li,[a] Michael J. Van Stipdonk,[c] Jonathan Martens,[d] Giel Berden,[d] Britta Redlich,[d] Jos Oomens,[d,e] Jun Li [a]*

***Abstract:*** Understanding of the nature and extent of bonding in uranyl–ligand bonding is crucial for the design of new ligands for nuclear waste separation and other applications. Among multiple-point-donor ligands, crown ethers are of increasing attention, which has burgeoned interest in the nature of uranyl–crown complexes. However, details of the bonding interaction between uranyl and 15-crown-5 are lacking. Here, we report a molecular uranyl–di-15-crown-5 complex featuring formal 6–fold An–O coordinating interactions. The results provide fundamental understanding of the coordination interaction of actinides with crown ether ligands, and provide a rational basis for ligand design in this area.

Uranyl–binding motifs are well known and offer distinctive handholds for the rational design of ligands that selectively bind uranyl.[1] Uranyl ion, with an overall charge of +2, has the ability to accommodate five or six equatorial donor ligand atoms in pentagonal or hexagonal bi-pyramidal geometry. This characteristic enables separation of uranyl from most alkali, alkaline and transition metals.[2] Although some uranyl binding motifs have been designed in organic ligands, and also appear in DNA and proteins, none has been able to go beyond the equatorial coordination threshold to achieve enhanced selectivity requirements.[3] Crown ether ligands have been employed as electron donors and as extractants for uranyl from aqueous media or from other species.[1b, 4] The selectivity of crown ethers can be attributed to cavity diameters that readily accommodate ions, and in the case of uranyl interactions between the high cation charge density and the crown oxygen sites. There have been several published experimental studies, including some crystal structures, for uranium(VI)−crown ether complexes. However, information about the structures of uranyl-crown ether complexes has been limited.[5] Studies of gas-phase complexes absent perturbation in condensed phases provides an opportunity to evaluate metal-ligand binding from an elementary perspective that illuminates key features. It was concluded based on hydration behaviour that in the gas-phase complex $UO_2(18C6)^{2+}$ the uranyl moiety inserts into the crown and is coordinated in the equatorial plane by the six oxygen donor sites [Ref. 1b]. This is rather different from the nature of this complex in aqueous solution where hydration effects destabilize the inclusion complex [Ref. 5]. An intriguing question is whether actinyl(VI) complexes having two crown ether complexes can be prepared and, if so, what is the structure of these complexes? Uranyl-di-crown ether complexes are essentially unexplored and provide an opportunity to elucidate at a fundamental level the complexation binding and selectivity of uranyl. In the present work the synthesis and IR spectrum of gas-phase $UO_2(15C5)_2^{2+}$ is reported, and the structure and bonding in this unique complex are evaluated by computational quantum chemistry.

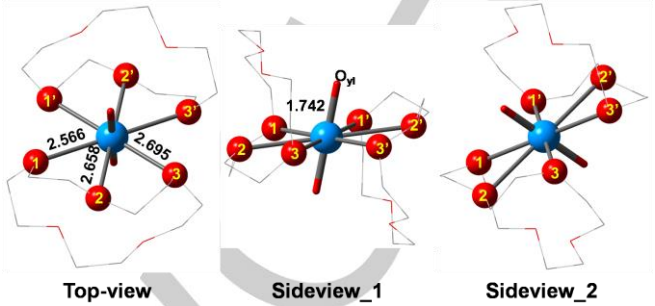


**Figure 1**. Optimized geometrical structure of Species A.

Theoretical insights at three different density functional levels (LDA,[7] PBE,[8] B3LYP,[9] M06[10] and M06-L[11]) have been employed. Since these calculations gave similar results, only geometries optimized at the PBE level are presented. There are four possible low-lying isomers for $UO_2(15C5)_2^{2+}$ stoichiometry from quantum chemical calculations (Figure S1). Species A, the theoretically optimized lowest-energy structure without imaginary frequencies, is shown in Figure 1. Structurally (Table S1), uranyl is trapped with six coplanar oxygen atoms in a Ci symmetry with U−$O_e$ bond lengths of 2.566 Å, 2.658 Å, 2.695 Å. Species B has six terminal U−$O_e$ bonded to the uranium atom; because of its slight Jahn-Teller distortion these six oxygen are not coplanar. Species C exhibits a chiral structure with $D_5$ symmetry, in which all ten of the crown oxygen atoms coordinate the uranium with a U−$O_e$ distance of 2.816 Å. The forth isomer, another sandwich bonding complex (species D), has two $O_e$ atoms terminal bonding to uranium with $C_{2h}$ symmetry. Species A is 8.1, 8.9 and 32.4 kcal/mol lower in energy than species B, C and D, respectively, at the PBE level of theory.

The experimental and computed IR spectra for species A are shown in Figure 1; those for species B, C and D are in Supporting Information. Species C and D can be eliminated based on significant disparities between the experimental and computed spectra. The B3LYP spectra for structurally similar species A and B are in rather good accord with the experimental spectrum. However, the peak splitting in the region of 1290 $cm^{-1}$ indicates species A, which is computed to be the ground state structure.

The infrared spectrum of $[UO_2(15C5)_2^{2+}]$ (Figure. 2) shows several strong bands at the range of 750 to 1100 $cm^{-1}$. The 844 $cm^{-1}$ band can be attributed to the vibrations of the weakly coordinated di-crown molecules, and is assigned to the antisymmetric $O_eUO_e$ stretching mode. The 976 $cm^{-1}$ band is in the U=O stretching frequency region and is assigned to the antisymmetric $O_{yl}UO_{yl}$ stretching mode of the linear $UO^{2+}$ core ion. The 1050 $cm^{-1}$ band is in the C−C stretching frequency region and is assigned to the antisymmetric C−C stretching mode of the crown. The 765, 920, 975 and 1006 $cm^{-1}$ bands are assigned to different vibrational modes of 15-crown-5 (Table S2), where the first two bands are attributed to C−O−C stretching

modes and the last two bands are assigned to C-C stretching modes, respectively. The absorptions at 886, 989 and 1098 $cm^{-1}$ at PBE and 848, 997 and 1058 $cm^{-1}$ at B3LYP match well the $O_eUO_e$ stretching mode, $O_{yl}UO_{yl}$ stretching mode and C-C stretching mode, respectively. The uranyl O=U=O asymmetric stretch frequency, $v_3$, is observed at 976 $cm^{-1}$. This is only slightly less red-shifted than the most extreme previously reported red-shift to 965 $cm^{-1}$ for a dipositive gas-phase uranyl complex [Ref. 1c]. This large red-shift of $v_3$ indicates substantial electron donation to the uranium metal center and a corresponding weakening of the uranyl bonds, consistent with the hexadentate equatorial oxygen coordination in species A. An interesting and unusual feature of species A is that the uranyl moiety is not perpendicular to the six-fold coplanar oxygen atoms. This distortion is attributed to steric repulsion between the uranyl oxygens and crown ether oxygens (Fig. 1, side view 1).

**Table 1.** Optimized geometrical structures, bond order, Mulliken charge and natural population analysis of $UO_2(15C5)_2^{2+}$.

| Bond Length | | Bond-orders | | Mulliken Charge | | | NPA | | |
|---|---|---|---|---|---|---|---|---|---|
| $U\text{-}O_{ax}$ (Å) | $U\text{-}O_e$(Å) | An - $O_{yl}$ | An - $O_e$ | q(An) | q($O_{yl}$) | q($O_e$) | q(An) | q($O_{yl}$) | q($O_e$) |
| 1.742 | 2.566,<br>2.658,<br>2.695,<br>3.703,<br>3.823 | 2.721 | 0.320<br>0.491<br>0.398<br>0.081<br>0.084 | 2.25 | -0.59 | -0.72<br>-0.72<br>-0.72<br>-0.74<br>-0.75 | 1.46 | -0.57 | -0.51<br>-0.54<br>-0.53<br>-0.53<br>-0.53 |

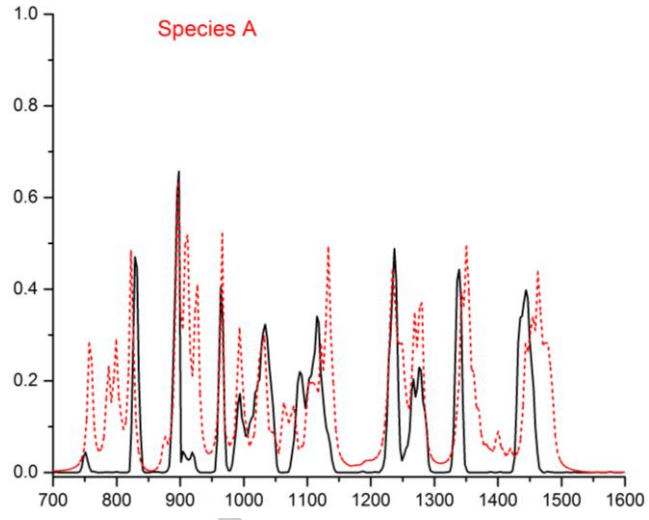


**Figure 2**. Experimental and B3LYP simulated IR spectra of the ground state $[UO_2(15C5)_2^{2+}]$ complex.

To comprehend the bonding between uranyl and the crown ether ligands of the $UO_2(15C5)_2^{2+}$, several bond analyses have been performed, such as bond orders by the Nalewajski-Mrozek (N-M)[12] method, Mulliken charges[13] and natural populations analysis (NPA)[14], energy decomposition approach (EDA)[15], the extended transition state method and the natural orbitals for chemical valence (ETS-NOCV)[16], Kohn Sham orbital interaction, natural localized molecular orbitals (NLMOs) analysis[17] and electron localization function (ELF)[18]. Obviously, the calculated N-M bond order (Table 1) of $U-O_e$ is four times smaller than those of $U-O_{yl}$, indicating weak covalent $U-O_e$ single-bonding interactions. In addition, Mulliken charge analysis shows that $O_e$ atoms gain negative charge via accommodation of uranyl.

The NLMOs analysis (Table S3) indicates one $\sigma^2\pi^2$ $U-O_e$ interaction. In the 15-Crown-5, each $O_e$ oxygen atom has two $C-O_e$ single bonds and two lone-pairs. Upon coordination to uranyl, there are covalent electron donations from the lone pairs to the 5f and 6d orbitals of uranyl, with the formation of weak σ and π bonding between $O_e$ atom and U atoms. This is consistent with the two dimensional ELF result shown in Figure 3.

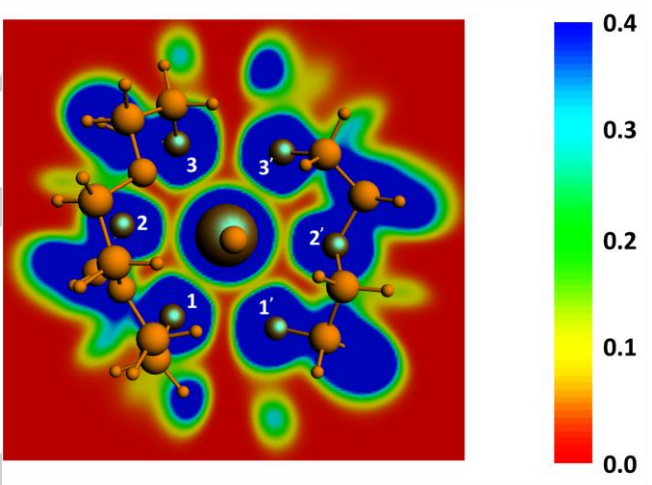


**Figure 3**. Two dimensional ELF contours for the O−U−O planes containing the U−O interactions. The results are based on the SR-ZORA calculated densities.

The EDA for $UO_2(15C5)_2^{2+} \rightarrow UO_2^{2+} + 2(15C5)$ results (Table S4) show that electrostatic and orbital interactions accounts for almost equal contributions to the total bonding energies, consistent with the bonding character of the $U-O_e$ bonds. Inspection of the Kohn Sham orbitals of $UO_2(15C5)_2^{2+}$ complexes (Figure S4) reveals that the bonding in the $U-O_e$ bonds mainly result from orbital interaction between $6d_\delta$, $5f_\delta$ and $5f_\phi$ orbitals of uranium and 2p orbitals of oxygen atoms in the crown ethers, which has been confirmed by additional ETS-NOCV analysis. ETS-NOCV analysis (Figure S5) further substantiates that the key bonding interactions between U and $O_e$ atoms are due to uranium 5f orbitals and 6d orbitals as the principal components of the σ and π bonding interactions, consistent with ther bond analyses.

In summary, comparison of experimental and computed IR spectra of the gas-phase $UO_2(15C5)_2^{2+}$ comlex indicate that it displays a distinctive 6-fold coplanar coordination structure that

could not be inferred from mass spectral results. Such a higly coordinated uranium center in uranyl is enabled by a structure in which the two 15C5 ligands each coordiante by three oxygen atoms but with minimal repulsive interaction. The strcture is further stabilized by an unusual non-perpendicular orientation of the uranyl moiety. Although each of the sic U–$O_e$ bonds is not particularly strong the overall bonding interaction is substantial, as indicated by an extreme red-shift in the uranyl asymmmetric stretch frequency. A juxtaposition of factors that include suitable coordination number of 15-crown-5 ether, the relative large electron density on the ligands, and the presence of available 5f and 6d acceptor orbitals create an unusually favorable ligand-field effect that results in substantial covalent bonding character, and electrostatic interactions that further significantly stabilize the coordination environent. The stabilization of this complex can be attributed to the unique bonding characteristics of a 5f-element.

Methodology Section

Experimental part:

The IRMPD experiments were performed at the Free Electron Laser for Infrared eXperiments (FELIX) Laboratory [Ref, Oepts, D.; van der Meer, A. F. G.; van Amersfoort, P. W. The Free-Electron Laser User Facility FELIX. *Infrared Phys. Technol.* **1995**, *36*, 297-308]. The $UO_2(15C5)_2^{2+}$ complex was produced by electrospray ionization (ESI) of a solution of ~100 μM uranyl perchlorate and ~ 400 μM 15-crown-5 (Sigma-Aldrich, 98%) in methanol (<10% water). The IRMPD spectra were acquired using a QIT/MS similar to that previously employed to study hydration of uranyl-crown complexes [Ref. 1b]. The QIT/MS has been modified [Ref. Kempkes, L. J. M.; Martens, J. K. M.; Grzetic, J.; Berden, G.; Oomens, J. Deamidation reactions of protonated asparagine and glutamine investigated by ion spectroscopy. *Rapid Commun. in Mass Spec.* **2016**, *30*, 483-490] such that the high-intensity tunable IR beam from FELIX can be directed into the ion packet, resulting in multiphoton dissociation that is appreciable only when the IR frequency is in resonance with an adequately high-absorption vibrational mode of the particular mass-selected complex being studied. The FEL produces ~5 μs long IR pulses with an energy of typically 40 mJ, which are in the form of a sequence of ~1-ps long micropulses at a 1 GHz repetition rate. The wavelength of the radiation was tuned between 6.2 and 14 μm in these experiments. The same IRMPD approach was recently employed to study organouranyl complexes [Ref. P. D. Dau, D. Rios, Y. Gong, M. C. Michelini, J. Marçalo, D. K. Shuh, M. Mogannam, M. J. Van Stipdonk, T. A. Corcovilos, J. K. Martens, J. Oomens, G. Berden, B. Redlich, J. K. Gibson, Synthesis and Hydrolysis of Uranyl, Neptunyl and Plutonyl Gas-Phase Complexes Exhibiting Discrete Actinide-Carbon Bonds, *Organometallics*, **2016**, *25*, 1228-1240].

**Computational methods:** The calculations were performed at the level of density functional theory (DFT) with relativistic corrections using the computational chemical software Gaussian 09 and ADF 2013.[19] The Supporting Information gives the full citations for the software. In searching for the ground state, the generalized gradient approximation (GGA) with the PBE functional and LDA with VWN functional. To balance between the accuracy and the time cost of the calculations, we applied Slater-type basis sets of valence triple-ζ plus two polarization function (TZ2P)[20] quality for U atom with the frozen core approximation to the inner shells with [$1s^2$-$2p^6$] for U and DZP for C and O with [$1s^2$]. The relativistic effects were accounted for by using scalar relativistic (SR) zero-order-regular approximation (ZORA)[21]. The nature of the optimized geometric structures on the potential energy surfaces was verified by analytical vibrational frequency analysis.

In order to avoid errors introduced by methods, hybrid-GGA (B3LYP), hybridmeta-GGA (M06), and local-meta-GGA (M06-L) methods were used to optimize the geometry and electronic structure with the Gaussian 09 code.[22] The quasi-relativistic small-core pseudo-potential ECP60MWB along with the corresponding ECP60MWB-SEG valence basis sets[23] was applied for uranium atom, and the aug-cc-pVTZ basis[24] for C, H and O atoms, which has been shown to provide reliable results for actinide systems. Vibrational frequencies were determined to check the minimum character of all structures. The Weinhold's natural bond orbitals (NBO) and natural localized MOs (NLMO) were performed at PBE/6-31g level on optimized geometries from PBE calculation in NBO 6.0 program.[25]

Further analyses of the results were performed with ADF 2013 on the PBE level. Energy decomposition analyses (EDA) were carried out by using combined Extended Transition State (ETS) with the Natural Orbitals for Chemical Valence (NOCV) theory to assess different orbital contributions to the total bonding energies.

**Acknowledgements**

This work was supported by the U.S. Department of Energy, Office of Basic Energy Sciences, Division of Chemical Sciences, Geosciences, and Biosciences, Heavy Element Chemistry program at LBNL under Contract No. DE-AC02-05CH11231 [J.K.G]; by start-up funds from the Bayer School of Natural and Environmental Sciences and Duquesne University [M.V.S.]; and by the Netherlands Organisation for Scientific Research (NWO) under vici-grant no. 724.011.002 and the Stichting Physica [J.O.].

**Keywords**: Uranyl Di-15-Crown-5 Complex • Electronic Structure • DFT• infrared spectroscopy

[1] a) C. Apostolidis, *Angew. Chem. Int. Ed.* **2010**, *49*, 6343–6347; b) Y. Gong, J. K. Gibson, *Inorg Chem* **2014**, *53*, 5839–5844; c) J. K. Gibson, H. S. Hu, M. J. Van Stipdonk, G. Berden, J. Oomens, J. Li, *J Phys Chem A* **2015**, *119*, 3366-3374.

[2] Y. Gong, H. S. Hu, L. F. Rao, J. Li, J. K. Gibson, *J Phys Chem A* **2013**, *117*, 10544-10550.

[3] a) J. H. Burns, J. R. Peterson, R. D. Baybarz, *J. Inorg. Nucl. Chem.* **1973**, *35*, 1171-1177; b) I. Castro-Rodriguez, *J Am Chem Soc* **2003**, *125*, 4565–4571; c) E. Galbis, *Angew. Chem. Int. Ed.* **2010**, *49*, 3811–3815; d) M. J. Polinski, *J Am Chem Soc* **2012**, *134*, 10682-10692; eB. A. Hess, *Phys Rev A* **1986**, *33*, 3742–3748; f) Y. L. Wang, Z. Y. Liu, Y. X. Li, Z. L. Bai, W.

Liu, Y. X. Wang, X. M. Xu, C. L. Xiao, D. P. Sheng, D. W. Juan, J. Su, Z. F. Chai, T. E. Albrecht-Schmitt, S. Wang, *J Am Chem Soc* **2015**, *137*, 6144–6147.

[4] a) C. J. Pedersen, H. K. Frensdor, *Angew Chem Int Edit* **1972**, *11*, 16-&; b) G. W. Gokel, W. M. Leevy, M. E. Weber, *Chem Rev* **2004**, *104*, 2723-2750.

[5] G. A. Shamov, G. Schreckenbach, R. L. Martin, P. J. Hay, *Inorg Chem* **2008**, *47*, 1465-1475.

[6] J. H. Lan, C. Z. Wang, Q. Y. Wu, S. A. Wang, Y. X. Feng, Y. L. Zhao, Z. F. Chai, W. Q. Shi, *J Phys Chem A* **2015**, *119*, 9178–9188.

[7] M. Gruning, O. V. Gritsenko, S. J. A. v. Gisbergen, E. J. Baerends, *J. Chem. Phys.* **2002**, *116*, 9591-9601.

[8] J. P. Perdew, K. Burke, M. Ernzerhof, *Phys. Rev. Lett.* **1996**, *77*, 3865-3868.

[9] A. D. Becke, K. E. Edgecombe, *J Chem Phys* **1990**, *92*, 5397-5403.

[10] Y. Zhao, D. G. Truhlar, *Theor. Chem. Acc.* **2008**, *120*, 215–241.

[11] Y. Zhao, D. G. Truhlar, *J. Chem. Phys.* **2006**, *125*, 1–18.

[12] a) A. Michalak, R. L. De Kock, T. Ziegler, *J. Phys. Chem. A* **2008**, *112*, 7256–7263; b) R. F. Nalewajski, J. Mrozek, *Int. J. Quantum Chem.* **1994**, *51*, 187–200; c) R. F. Nalewajski, J. Mrozek, A. Michalak, *International Journal of Quantum Chemistry* **1997**, *61*, 589–601.

[13] R. S. Mulliken, *J. Chem. Phys.* **1955**, *23*, 1833–1840.

[14] F. Martin, H. Zipse, *J. Comput. Chem.* **2005**, *26*, 97–105.

[15] L. Deng, T. Ziegler, *Int. J. Quantum Chem.* **1994**, *52*, 731–765.

[16] a) A. Michalak, M. Mitoraj, T. Ziegler, *J. Phys. Chem. A* **2008**, *112*, 1933–1939; b) M. Mitoraj, A. Michalak, *J. Mol. Model.* **2007**, *13*, 347–355; c) T. Ziegler, A. Rauk, *Theoret. Chim. Acta* **1977**, *46*, 1–10.

[17] A. E. Reed, L. A. Curtiss, F. Weinhold, *Chem Rev* **1988**, *88*, 899-926.

[18] P. de Silva, J. Korchowiec, T. A. Wesolowski, *ChemPhysChem* **2012**, *13*, 3462–3465.

[19] E. J. Baerends, D. E. Ellis, P. Ros, *Chem. Phys.* **1973**, *2*, 41-51.

[20] E. van Lenthe, E. J. Baerends, *J. Comput. Chem.* **2003**, *24*, 1142–1156.

[21] E. van Lenthe, E. J. Baerends, J. G. Snijders, *J. Chem. Phys.* **1993**, *99*, 4597.

[22] M. Frisch, W. C. et al. Gaussian, 2010, see http://www.gaussian.com.

[23] a) M. Dolg, U. Wedig, H. Stoll, H. Preuss, *J. Chem. Phys.* **1987**, *86*, 866–872; b) X. Cao, M. Dolg, *J. Molec. Struct. (THEOCHEM)* **2004**, *673*, 203-209; c) X. Cao, M. Dolg, H. Stoll, *J Chem Phys* **2003**, *118*, 487-497.

[24] a) D. E. Woon, T. H. Dunning Jr., *J. Chem. Phys.* **1993**, *98*, 1358–1371; b) R. A. Kendall, T. H. Dunning Jr., R. J. Harrison, *J. Chem. Phys.* **1992**, *96*, 6796–6806.

[25] A. E. Reed, R. B. Weinstock, F. Weinhold, *J. Chem. Phys.* **1985**, *83*, 735–746.

**Entry for the Table of Contents**

**AFFILIATIONS**

[a] Dr. S. Hu, Dr. W.-L. Li, Prof. Dr. J. Li
Department of Chemistry and Key Laboratory of Organic Optoelectronics & Molecular Engineering of Ministry of Education, Tsinghua University, Beijing 100084 (China), E-mail: junli@tsinghua.edu.cn

[b] Dr. J. K. Gibson
Chemical Sciences Division, Lawrence Berkeley National Laboratory, Berkeley, California 94720, United States, E-mail: jkgibson@lbl.gov

[c] Prof. Dr. M. J. Van Stipdonk
Department of Chemistry and Biochemistry, Duquesne University, Pittsburgh, Pennsylvania 15282 United States

[d] Dr. J. Martens, Dr. G. Berden, Dr. B. Redlich, Prof. Dr. J. Oomens
Radboud University, Institute for Molecules and Materials, FELIX Laboratory, Toernooiveld 7c, 6525ED Nijmegen, The Netherlands

[e] Prof. Dr. J. Oomens
van't Hoff Institute for Molecular Sciences, University of Amsterdam, Science Park 904, 1098XH Amsterdam, The Netherlands

Supporting information for this article is given via a link at the end of the document.